UNIVERSITY OF HELSINKI REPORT SERIES IN PHYSICS

HU-P-D134

Sticking and erosion at carbon-containing plasma-facing materials in fusion reactors

Petra Träskelin

Accelerator Laboratory
Department of Physical Sciences
Faculty of Science
University of Helsinki
Helsinki, Finland

ACADEMIC DISSERTATION

To be presented, with the permission of the Faculty of Science of the University of Helsinki, for public criticism in the Small Auditorium E204 of the Department of Physical Sciences (Physicum), on August 26th, 2006, at 10 o'clock a.m.

HELSINKI 2006

ISBN 952-10-2124-1 (printed version)
ISSN 0356-0961
Helsinki 2006
Helsinki University Printing House (Yliopistopaino)

ISBN 952-10-2125-X (PDF version)
http://ethesis.helsinki.fi/
Helsinki 2006
Electronic Publications @ University of Helsinki (Helsingin yliopiston verkkojulkaisut)

Petra Träskelin: **Sticking and erosion at carbon-containing plasma-facing materials in fusion reactors**, University of Helsinki, 2006, 31 p.+appendices, University of Helsinki Report Series in Physics, HU-P-D134, ISSN 0356-0961, ISBN 952-10-2124-1 (printed version), ISBN 952-10-2125-X (PDF version)

Classification (INSPEC): A3410, A7920N
Keywords (INSPEC): Molecular dynamics, ion-surface impact, plasma-facing material, sticking, erosion

ABSTRACT

Controlled nuclear fusion is one of the most promising sources of energy for the future. Before this goal can be achieved, one must be able to control the enormous energy densities which are present in the core plasma in a fusion reactor. In order to be able to predict the evolution and thereby the lifetime of different plasma facing materials under reactor-relevant conditions, the interaction of atoms and molecules with plasma first wall surfaces have to be studied in detail. In this thesis, the fundamental sticking and erosion processes of carbon-based materials, the nature of hydrocarbon species released from plasma-facing surfaces, and the evolution of the components under cumulative bombardment by atoms and molecules have been investigated by means of molecular dynamics simulations using both analytic potentials and a semi-empirical tight-binding method.

The sticking cross-section of CH_3 radicals at unsaturated carbon sites at diamond (111) surfaces is observed to decrease with increasing angle of incidence, a dependence which can be described by a simple geometrical model. The simulations furthermore show the sticking cross-section of CH_3 radicals to be strongly dependent on the local neighborhood of the unsaturated carbon site.

The erosion of amorphous hydrogenated carbon surfaces by helium, neon, and argon ions in combination with hydrogen at energies ranging from 2 to 10 eV is studied using both non-cumulative and cumulative bombardment simulations. The results show no significant differences between sputtering yields obtained from bombardment simulations with different noble gas ions. The final simulation cells from the 5 and 10 eV ion bombardment simulations, however, show marked differences in surface morphology. In further simulations the behavior of amorphous hydrogenated carbon surfaces under bombardment with D^+, D_2^+, and D_3^+ ions in the energy range from 2 to 30 eV has been investigated. The total chemical sputtering yields indicate that molecular projectiles lead to larger sputtering yields than atomic projectiles.

Finally, the effect of hydrogen ion bombardment of both crystalline and amorphous tungsten carbide surfaces is studied. Prolonged bombardment is found to lead to the formation of an amorphous tungsten carbide layer, regardless of the initial structure of the sample. In agreement with experiment, preferential sputtering of carbon is observed in both the cumulative and non-cumulative simulations.

Contents

1 INTRODUCTION

The world energy consumption is continuing to increase. The reasons are obvious: the modern society in industrialized countries depends on energy supplies, the world population is growing, and the industrialization of developing countries is demanding increasing amounts of energy.

Today, the primary energy source is the burning of fossil fuels such as coal, oil, and gas [1]. There are many problems related to the use of these fossil fuels, such as the release of carbon dioxide upon their combustion, and the limited amount of exploitable geological resources.

A small part of the energy produced on earth comes from nuclear power plants and alternative energy sources (i. e. solar, wind, biomass). Although it is presumed that the technology of renewable energy sources will develop, there are no indications that these sources will be able to satisfy the total demand in the future.

An alternative source of energy is thermonuclear fusion. As a matter of fact, similar processes are the primary source of solar energy. At the core of the sun the temperatures and pressures are high enough for fusion to occur among light elements such as hydrogen, whereby an enormous amount of energy is released. Fusion research aims to reproduce these processes in a controlled fashion. In comparison with fossil fuel and nuclear (fission-based) power production, fusion technology is environmentally safe and no long-term storage of radioactive waste is required. Moreover, the fuel needed for fusion, namely deuterium and lithium, is accessible in large amounts almost everywhere on earth providing a practically inexhaustible source of energy.

In a tokamak fusion reactor, the fusion plasma is controlled by magnetic fields and confined in the center of a toroidal vessel. During device operation, some of the plasma particles leak outside the closed magnetic field lines and interact with the chamber walls. In tokamaks, specially designed chamber wall structures are used to handle the boundary plasma. The term ’first wall’ is used to distinguish the plasma-facing armor material from the actual walls of the vacuum chamber. The resulting intense ($\sim 10^{22}$ - 10^{24} ions/m^{2}s) bombardment by hydrogenic particles causes severe damage of the first wall, leading to the erosion of the plasma facing components (PFC), degradation of their thermal and mechanical properties, and deposition of radioactive tritium in the wall structures [2; 3; 4; 5]. The fusion plasma purity, on the other hand, will be compromised as eroded impurity species from the PFCs enter the plasma and dilute it. In addition, radiation losses, which are proportional to the atomic number Z of the impurity species, lead to cooling of the plasma and the extinction of the fusion reaction.

The selection of materials for the plasma-facing components is, therefore, crucial for the development of commercially viable fusion technology.

During the last decades, carbon was considered to be one of the most promising first wall materials. Carbon has excellent thermal and mechanical properties, but chemical erosion by oxygen, and more importantly hydrogen atoms and ions, results in too high erosion rates for long-term operation [6], which constitutes a major problem. Moreover, hydrocarbon species released from the first wall surfaces form hydrocarbon films containing tritium upon redeposition. This leads to the accumulation of a harmful tritium inventory in the vessel walls. Strategies to circumvent these limitations are currently intensively investigated. For instance, the introduction of dopants aims to reduce the tritium retention and chemical sputtering by hydrogen and oxygen while at the same time retaining the required thermo mechanical properties.

Further research is also needed in order to be able to predict the evolution and thereby the lifetime of different PFC materials under reactor relevant conditions. In this respect, the fundamental sticking and erosion processes of carbon-based materials, the nature of hydrocarbon species released from plasma-facing surfaces, and the evolution of the components under cumulative bombardment of atoms and molecules deserve particular attention.

2 PURPOSE AND STRUCTURE OF THIS STUDY

The purpose of this thesis is to improve the understanding of sticking processes and the erosion of fusion plasma facing materials. The results aid in the selection and development of fusion reactor materials.

This thesis consists of the summary below and five publications — printed, accepted, or under review — in international peer-reviewed journals. These publications are referred to in bold face Roman numbers and are included after the summary.

The structure of the summary is as follows. In this section a brief overview of all the publications is given, as well as a clarification of the author's contribution to these. The necessary basic concepts and the background of the results reported in this thesis are given in section 3. In section 4 an overview of the methods used to obtain the results is given. The results from simulations on methyl radical sticking onto diamond (111) surfaces are presented in section 5. In section 6 results from simulations on carbon erosion are presented. The thesis is summarized in section 7.

2.1 Summaries of the original publications

In publication **I** the sticking of methyl (CH_3) radicals onto unsaturated carbon sites was investigated with respect to the effect of the local neighborhood of the dangling bond. The research on CH_3 radical sticking was continued in publication **II**, where the angular dependence was investigated and a simple geometrical model was developed capable of explaining the simulation data. The effect on amorphous hydrocarbon surfaces under hydrogen and He, Ne, and Ar impurity ion bombardment was investigated in publication **III**. In publication **IV** the carbon erosion yields from hydrocarbon surfaces under deuterium atom and molecule bombardment were compared. Carbon erosion from both crystalline and amorphous tungsten carbide surfaces was investigated in publication **V**.

Molecular dynamics simulations, employing both quantum mechanical (publications **I** and **II**) and empirical force models (all publications), were used in these studies.

Publication I: Molecular dynamics simulations of CH_3 sticking on carbon surfaces, P. Träskelin, E. Salonen, K. Nordlund, A. V. Krasheninnikov, J. Keinonen and C. H. Wu, *Journal of Applied Physics* **93**, 1826-1831 (2003).

> In this study sticking cross sections for CH_3 radical chemisorption on unsaturated carbon sites were obtained. It was shown that the chemisorption of a CH_3 radical at a dangling bond is highly affected by the local neighborhood of the unsaturated carbon atom site. Sticking cross sections of a totally bare dangling bond site at the surface and a site partly shielded by neighboring methyl groups were observed to differ by two orders of magnitude.

Publication II: Molecular dynamics simulations of CH_3 sticking on carbon surfaces, angular and energy dependence, P. Träskelin, E. Salonen, K. Nordlund, J. Keinonen, and C. H. Wu, *Journal of Nuclear Materials* **334**, 65-70 (2004).

> In this study sticking cross sections for CH_3 radicals at different angles of incidence and different energies were calculated. The chemisorption of a CH_3 radical at 2100 K onto a dangling bond was found to be highly dependent on the angle of incidence of the incoming radical. The angular dependence was explained with a simple geometrical model. The sticking of CH_3 radicals with higher kinetic energies (1, 5 and 10 eV) was studied both for a fully hydrogen terminated surface and a surface with a single dangling bond.

Publication III: H, He, Ne, Ar-bombardment of amorphous hydrocarbon structures, P. Träskelin, K. Nordlund, and J. Keinonen, accepted for publication in *Journal of Nuclear Materials* (2006).

In this study both non-cumulative and cumulative bombardment simulations were performed of hydrogen, helium, neon and argon ions impinging onto amorphous hydrocarbon surfaces at energies ranging from 2 to 10 eV. The investigation revealed no significant differences between the sputtering yields of different noble gas ions. A marked difference in the surface morphology was, however, observed between the final simulation cells from the simulations with 5 and 10 eV ion bombardment.

Publication IV: Methane production from ATJ graphite by slow atomic and molecular D ions: evidence for projectile molecule-size-dependent yields at low energies, L. I. Vergara, F. W. Meyer, H. F. Krause, P. Träskelin, K. Nordlund, and E. Salonen, accepted for publication in *Journal of Nuclear Materials* (2006).

In this study total chemical sputtering yields were obtained for D^+, D_2^+, and D_3^+ ions at energies of 1 – 30 eV impinging onto hydrocarbon surfaces. The resulting yields indicate that molecular projectiles lead to larger yields per atom than atomic projectiles.

Publication V: Hydrogen bombardment simulations of tungsten-carbide surfaces, P. Träskelin, N. Juslin, P. Erhart, and K. Nordlund, submitted to *Physical Review B* (2006).

In this study, the behavior of crystalline as well as amorphous tungsten carbide surfaces under hydrogen bombardment was investigated. It was found that prolonged bombardment leads to the formation of an amorphous tungsten carbide layer. Larger sputtering yields were obtained from carbon-terminated surfaces than from tungsten-terminated surfaces. In agreement with experiment, carbon was observed to be sputtered preferentially, both in the cumulative and non-cumulative simulation runs.

2.2 Author's contribution

The author carried out all the calculations, performed the analysis of the results, and wrote most of the text of publications **I**, **II**, **III**, and **V**. In publication **IV** the author ran the simulations, analyzed the simulation results, and edited all parts of the final publication. The experimental work in this publication was carried out by a collaborating group.

3 FUSION REACTOR PLASMA-FACING MATERIALS

In this section advantages and disadvantages of different materials to be used for plasma facing components are reviewed. Basic interaction mechanisms at the first wall and divertor are outlined. Finally current problems with plasma facing components in next-step fusion experiments are addressed.

3.1 Carbon, tungsten and beryllium

The first successful deuterium-tritium burning experiment was conducted in the Joint European Torus (JET) which employed beryllium and carbon as plasma-facing materials. In present day tokamaks, typically different types of graphite or carbon fiber composites are used.

Carbon-based materials are in many ways ideal as plasma facing materials. They feature high thermal conductivities, excellent thermal shock resistance, and do not melt (the sublimation point of graphite is $\sim$ 3640 K) [7]. Carbon is a low activation material and its low atomic number (Z) makes it possible to tolerate much higher carbon impurity concentrations in the core plasma compared to high-Z materials like tungsten. A low concentration of carbon in the divertor region plasma, aids in cooling the edge plasma. The use of carbon, however, has some drawbacks. Erosion of plasma facing components, tritium retention in redeposited layers, and contamination of the core plasma by sputtered materials are the main problems. In addition, volatile molecules, such as CO and CO_2, are formed efficiently due to carbon etching by oxygen, the main intrinsic impurity in the vacuum chamber. Estimates of the erosion rates in fact indicate too short operational times for carbon plasma facing components in actual reactors [6; 8]. From both simulations and experimental results, it can be concluded that the chemical erosion of carbon-based materials remains a problem which is very difficult to solve.

Due to its low physical sputtering yield and good thermal properties, tungsten is among the main candidates for plasma-facing materials in fusion devices both at the first wall and in the divertor region. While the erosion of tungsten under hydrogen bombardment is negligible, several other mechanisms, however, can contribute to tungsten erosion in fusion device, for example blistering [9], and sputtering of redeposited tungsten species [10; 11], which could be enhanced due to lowering of the threshold energy of sputtering by oxygen [12]. Due to the large atomic weight, tungsten ions are much more harmful plasma impurities than carbon or beryllium ions.

Beryllium, on the other hand, is very light, but has a very high erosion rate [13] under tokamak-relevant conditions, and melts easily. The usefulness of beryllium as a first wall material is based on its low atomic number, its ability to remove oxygen from the plasma, and its ability to pump hydrogen

almost continuously during short discharges. This hydrogen pumping occurs in spite of the extremely low equilibrium solubility of hydrogen isotopes in beryllium.

The first tokamak of the next generation, the International Thermonuclear Experimental Reactor (ITER), is expected to give a clear proof of the feasibility of fusion-based power production [1; 8]. The current ITER design involves carbon-based materials only in the high heat flux components, while tungsten and beryllium will be used elsewhere in the divertor and the first wall [1].

3.2 Tokamak plasma facing components

In tokamak devices the fusion plasma is confined in a toroidal vacuum chamber by the superposition of magnetic fields. The confinement properties in tokamaks are excellent, but some of the plasma particles can escape the magnetic confinement and interact with the vessel walls. This leads to enormous thermal and particle loads at the surfaces of the plasma facing parts. Special components, namely limiters and divertors are used to control the particle flux.

The purpose of a divertor in a tokamak-like fusion reactor is to be the target for particle exhaust and redirect impurities into regions remote from the core plasma. Before reaching the target plates, the density of the plasma increases and the plasma cools down, reducing the power load. Further cooling of the plasma can be achieved by puffing a small amount of gas (e.g. Ne, Ar) in the plasma above the divertor plates.

Since the plasma electrons have higher velocities than the ions, they reach the divertor target plates faster. This results in a negative surface charge on the plates, creating an electric field [14]. Before impinging on the divertor plates, the plasma ions are accelerated by this electric field, the sheath, leading to an energy distribution which corresponds roughly to a shifted Maxwellian distribution.

The ions are neutralized by the excess electrons at the surface upon reaching the target plates, and the neutralized plasma species and impurities released from the target plates are finally pumped off from the vacuum chamber. The pumping is essential, as the impurity species can enter the core plasma with deteriorating effects. The impurity species can also be ionized in collisions with the plasma electrons, and redeposited by the sheath.

3.3 Carbon drift and redeposition

Continuing high-flux bombardment by hydrogen ions and neutrals onto carbon-based materials leads to the formation of amorphous hydrogenated carbon (a-C:H) structures at the surface of the divertor

plates [14]. During this process, hydrocarbon species are sputtered, transported and redeposited onto the fusion first walls. It is known that the eroded species from carbon plasma-facing components form hydrocarbon films not only on the divertor plates, where prompt redeposition takes place, but also in other parts of the vacuum chamber [15]. Tritium is rather strongly bound in these hydrocarbon films, leading to the accumulation of tritium in the first wall structures. Tritium is highly radioactive and cannot be recycled easily. A major issue in fusion devices is therefore achieving good control over the tritium inventory bound in these deposited hydrocarbon films.

3.4 Current problems

The plasma-facing component lifetime and the contamination of the plasma is primarily determined by the erosion and the chemisorption rates and mechanisms of the plasma-facing material. Detailed investigations over erosion and sticking processes of these materials are hence of great importance.

For polymer-like hydrocarbon films studied in radical beam experiments, it has been shown that an additional flux of atomic hydrogen can enhance the sticking coefficient of CH_3 by two orders of magnitude. The hydrogen flux provides new adsorption sites via abstraction of H_2 molecules. The results clearly show the importance of unsaturated carbon sites for the sticking of methyl radicals. Employing various experimentally determined parameters, the cross section of methyl radical chemisorption on an unsaturated carbon site has been obtained to be 2.4 $Å^2$ from rate equations [16; 17; 18]. If the elimination of hydrogen due to adsorption of methyl is, however, properly taken into account, the cross section is calculated to be larger. The cross section obtained for methyl radicals at normal incidence, σ_c = 11 $Å^2$, is larger than the average size of a surface site (7.4 $Å^2$). A simple geometrical argument is therefore insufficient to explain the large cross section. The result obtained in these investigations for methyl radicals at 45° angle of incidence, σ_c = 5.9 $Å^2$, was shown to be in excellent agreement with experiments, but smaller than the average size for a surface site. In order to successfully model and predict the performance of the next-step device, detailed investigations need to be carried out in order to understand these puzzling results.

Experiments carried out at the ASDEX Upgrade resulted in the formation of both soft polymer-like C:H films (H/C $\sim$ 1) and hard C:H films (H/C $\sim$ 0.4). Also in this case, a detailed knowledge of the chemistry at the surface is of fundamental importance. Elementary erosion and re-deposition parameters for hydrocarbon species, such as the angular dependence of the sticking cross section, are still missing.

The carbon plasma facing components will suffer significant chemical erosion and sputtering by low energy hydrogen ion impact during device operation, which to a large extent determines the lifetime

of a component. Due to evolving divertor design, the interest in the erosion characteristics of the carbon surfaces is shifting to progressively lower impact energies. Many studies of chemical sputtering of graphite with low energy beams have been reported. The fluxes of atomic beams are lower than for molecular beams. Since the yield decreases with decreasing energy, the low flux of atomic beams limits the reliability of experiments at energies below 30 eV/D. The studies mentioned above, therefore, employed molecular beams and then quoted the sputtering yields for incident H or D atoms at energies obtained by dividing the impacting molecular projectile kinetic energy by the number of constituent H or D atoms. This is equivalent to the assumption that atomic and molecular projectiles at the same energy per D atom lead to the same sputtering yield per atom in the investigated energy range. Further studies are needed in order to examine the validity of this approximation for carbon sputtering by atomic D^+ and molecular D_x^+ ions impacting on graphite surfaces at room temperature.

Metal carbides are naturally present at the interfaces between the carbon first wall and the metallic parts underneath. Moreover, they can also be formed when hydrocarbon molecules, eroded under particle bombardment, react with metal parts in other sections of the plasma chamber. Because of the abundance of tungsten, the most relevant metal carbide to be considered in this context is WC. Sputtering yields in WC have been measured by a few groups [19; 20; 21; 22; 23]. The results show that preferential sputtering of carbon plays an important role for the erosion of tungsten carbide [19], and that at least part of the sputtering is of chemical origin [20]. However, the binary collision approximation (BCA) simulations used until now to analyze the experimental results capture neither chemical sputtering nor the details of surface structure changes. Understanding the interaction of hydrogen plasmas with WC is particularly important since the divertor armor in ITER is designed to consist at least partially of carbon coated tungsten.

4 METHODS

Modeling studies can provide valuable insight on erosion and sticking under atom and molecule bombardment. At energies below the regime of physical sputtering, it is clear that the methods used have to provide a realistic description of the intricate chemistry of hydrocarbon radicals, noble gases (such as those investigated in this thesis, namely He, Ne, and Ar), and hydrogenic ions, interacting with hydrocarbon and tungsten-carbide surfaces. This rules out the use of models based on the BCA [24], which are otherwise widely used for simulating irradiation of materials, with high-energy ions.

The results presented in this thesis have been obtained by means of the molecular dynamics (MD) simulation method which is described in the following section.

Molecular dynamics simulations require models which are capable of providing energies and forces for arbitrary atomic configurations. In this thesis two different methods were employed: (1) The majority of results were obtained using analytical inter atomic potentials. The Brenner hydrocarbon potential [25] was used for modeling carbon surfaces (publications **I**, **II**, **III**, and **IV**) while the simulations of tungsten carbide surfaces (publication **V**) were based on an analytical bond-order potential. (2) The tight-binding method in the formulation by Porezag *et al.* [26; 27] was employed in the study of methyl radicals sticking on carbon surfaces (publications **I** and **II**) in order to capture quantum-mechanical effects.

4.1 Molecular dynamics

The molecular dynamics method is an excellent tool for studying processes on the atomic scale. In particular for studies of far-from-equilibrium processes, such as atom cascades resulting from ion irradiation, where the applicability of analytical methods is sometimes questionable, MD simulations can provide valuable insight. Since the first implementations of the method in the late 1950ies [28]. the accuracy and speed of MD simulations increased continuously with the rapid development of computer technology.

In MD simulations the motion of an ensemble of atoms is followed by solving the equations of motion for each atom. Since an analytic solution is not possible for more than three particles, this is achieved by discretizing Newton's equations and application of numerical integration methods. In order to avoid violation of the energy conservation, the discretization interval (time step) has to be kept sufficiently small, typically of the order of about 1 fs. This practically limits the maximum simulation time achievable to nanosecond time scales. Especially in simulations involving energetic particles, too abrupt changes in the atom positions may lead to unphysical behavior. For the best computational efficiency in the calculations, a variable time step length may be used [29].

MD methods can be roughly divided into two categories, classical and quantum-mechanical, depending on the force model used. In classical MD, the inter atomic forces are derived from some potential energy function. The potentials are fitted to data from quantum-mechanical calculations and/or experiment, such as the melting point, elastic constants, bond lengths, and energies. Electronic effects are not explicitly included in classical MD.

The advantage of the classical models is their efficiency, since the computational time scales practically linearly with the number of atoms in the simulation. A typical system size for a classical MD simulation is of the order of 10^3 - 10^7 atoms. Non-local effects, which take into account the bonding structure at non-nearest neighbor atoms, can be included in the potential to improve the accuracy of

the calculations. This is especially important in the case of carbon, where heterogeneous bonding configurations arise from the mixture of sp^2- and sp^3-hybridized bonding.

Quantum-mechanical models range from *ab initio* to more efficient semi-empirical methods. The energy of a system of atoms is calculated by iteratively solving the Schrödinger equation, with some approximations. While the calculations are physically better motivated than in the classical models, they are also computationally much more demanding. Hence, the size of a system studied is usually restricted to $\sim 2 - 100$ atoms.

4.2 Brenner empirical hydrocarbon potential

The reactive bond-order hydrocarbon potential developed by Brenner [25] was used in several papers of this thesis. The potential is a modified Tersoff-type potential [30; 31], augmented with continuous bond-order correction functions. The parameters of this potential were fitted to a large data base comprising data on bulk carbon structures and small hydrocarbon molecules from both experimental and first-principles calculations [25].

As the inter atomic forces in covalently bonded materials weaken rapidly with increasing distance, the calculations can be sped up by imposing a maximum interaction distance (cutoff radius) for each combination of atom types in the simulations. All atoms outside the cutoff radius are neglected when calculating the force acting on a given atom. The Brenner potential provides a reasonably realistic description of various pure carbon structures and hydrocarbon molecules, as well as dynamic effects, such as bond forming and breaking. Hence, it has been used for various studies of carbon and hydrocarbon systems [32; 33; 34; 35]. Some problems with the potential, however, have been identified in the past. Firstly, the structures given by the potential for dense amorphous carbon have been shown to contain too small fractions of sp^3-bonded carbon [36]. Secondly, it has also been observed that the chemical sputtering of carbon (at least from the very surface) is sensitively dependent on the C-C interaction range of the potential [37]. In publication **I**, the sticking probabilities of methyl radicals on unsaturated carbon sites when calculated using the Brenner potential are shown to be much smaller than those obtained by tight-binding calculations and experiments. This is particular noteworthy since the potential was originally developed for the growth of diamond via chemical vapor deposition. In all of these cases, the performance of the potential can be significantly improved by increasing the maximum C-C interaction range of the potential without deteriorating other essential properties. In order to present the interaction between the noble gas atoms (He, Ne, and Ar) and the hydrocarbon target, pair potentials of the Ziegler-Biersack-Littmark (ZBL) [38] type were employed.

4.3 W–C–H potential

In order to model the complex interactions in the W–C–H system, we employed a recently developed reactive bond-order potential which is capable of describing both the pure and the compound phases at a high level of precision [39].

In this model, Brenner's hydrocarbon potential is combined with parameter sets for W–W, W–C, and W–H interactions. The model has been adjusted to reproduce experimental and first-principles data on various structures with different local atomic coordinations. It has also been successfully validated in several test cases which were not explicitly included in the fitting database, which provides confidence that the potential is well suited for simulations of hydrogen and hydrocarbon interactions with tungsten. It also represents a possibly general route for modeling metal carbides.

4.4 Tight-binding method

The tight-binding (TB) method [40] is a relatively efficient quantum-mechanical method. It is based on the assumption that the total energy in an atomic system can be approximated as the sum of two terms: a repulsive pairwise inter atomic potential, which describes the contribution of the core electrons of atoms, and the band energy, which captures the cohesion due to the interaction of the valence electrons. The former term is usually fitted to experimental data, making the method in fact semi-empirical. The latter term is calculated by solving the Schrödinger equation for the electrons in the field of the atom cores, with the Hamiltonian replaced by a parametrized matrix. A set of basis functions, usually having the same symmetry properties as the atomic orbitals, is then used to describe the valence electron states.

The method has been shown to give a qualitatively correct description of various covalently bonded materials, in particular amorphous carbon [41; 42]. Due to a number of (physically motivated) approximations, the method is quite fast compared to first-principles methods such as density-functional theory or Hartree-Fock. This enables the study of larger systems and collecting at least moderate statistics for atomic processes. While carbon sputtering yields by low-energy hydrogen are still too low for comprehensive sputtering studies with the TB method, the quantum mechanical treatment can still give a physically more accurate description of the chemical bond breaking than the classical methods. In turn, it is, thereby, possible to assess the reliability of the analytic potential calculations discussed above.

4.5 Modeling of ion bombardment on carbon cells

The ion bombardment simulations were carried out with the HCPARCAS simulation code, developed by K. Nordlund at the Accelerator Laboratory. The program is especially tailored to simulate far-from-equilibrium phenomena, such as cascades produced by irradiation.

4.5.1 Types of simulation cells

Publications **I** and **II** describe a detailed investigation of sticking of methyl radicals on diamond (111) surfaces. Due to the use of the TB method, which was used to complement the Brenner potential, the simulation cells comprised only 173 to 183 atoms. In total four different diamond (111) surfaces were created for our investigations, featuring (a) one unsaturated carbon site, (b) seven unsaturated carbon sites, (c) one unsaturated carbon site on top of a cluster consisting of ten atoms on the diamond (111) surface, and (d) one unsaturated carbon site surrounded by three methyl methyl groups.

Under intense hydrogen irradiation carbon PFC surfaces eventually amorphize. Therefore, in publications **III** and **IV** of this thesis random hydrocarbon networks were investigated. To this end, amorphous hydrogenated carbon (a-C:H) cells with about 1000 atoms were created by repeated temperature and pressure treatment employing the Berendsen thermostat and barostat [43]. The final surface densities were approximately 2.4 g/cm^2, and the fraction of three- and four-fold coordinated carbon atoms ranged from 60 to 70 % and 25 to 40 %, respectively.

In paper **V**, both crystalline and amorphous tungsten-carbide surfaces were considered. In the amorphous cells, which in total contained about 1000 atoms, the carbon content varied between 10 and 50 %. These cells comprised 1920 atoms. For the crystalline tungsten-carbide cells, both carbon ((0001)-C) and tungsten ((0001)-W) terminated surfaces were created.

4.5.2 Bombardment species

Although the term 'ion' is used here to distinguish the incident atom from the target atoms, conventional classical MD simulations do not describe the charge transfer reactions between the atoms. Thus, all the atoms in the simulation including the impinging one are in fact neutrals. This is not a major restriction for the modeling, as the ions impinging on the divertor plates in tokamaks will be promptly neutralized by the excess electrons at the surface.

In the series of impact simulations, the impinging species were assigned either fixed kinetic energies or random energies according to a Maxwellian distribution. The former approach allowed the study

of the chemical sputtering as a function of the energy. It is often better suited for comparison with laboratory experiments, where almost mono energetic ion beams are used. The latter approach corresponds to the conditions of hydrogen bombardment of carbon plasma facing materials in tokamaks, where the incident energies follow approximately Maxwellian distributions.

Two types of irradiation simulations were carried out: cumulative and non-cumulative. In non-cumulative simulations, the same initial surface is used for all impact events in a series of simulations, which puts the focus on the probabilities for certain surface processes. In cumulative simulations, on the other hand, after each bombardment step the simulation cell was cooled and subsequently subjected to the next bombardment event. Thereby, it was possible to study the evolution of the surface structure subjected to a fluence of incoming particles.

5 STICKING

In this section, a summary over the results obtained from the investigations of methyl radical sticking on diamond (111) surfaces will be given. These studies are presented in publications **I** and **II**. The most important findings are the sensitivity of the local neighborhood of an unsaturated carbon site on the sticking cross section, and the angular dependence of an incoming methyl radical on the sticking cross section. At the end of the section, possible radical – dangling bond reaction mechanisms are discussed.

The effective sticking cross section, σ_c, of hydrocarbon radical chemisorption on unsaturated carbon atom sites can be defined as an area on the surface to which the radical always chemisorbs upon impact, since the growth of the carbon matrix by CH_3 proceeds only via chemisorption on these sites. Factors contributing to σ_c are not only the feed gas and substrate surface temperature [44], but also the local atomic neighborhood of the adsorption sites, and the angular dependence of the incoming radicals [16; 17; 18]. Provided that the cross section is known, along with the concentration of adsorption sites, n_{db}, the sticking coefficient of the growth species s and hence the overall growth of C:H films can be predicted. Moreover, provided that the dangling bond coverage of the surface is low enough, each CH_3 impact near a dangling bond site can be described independently of the other dangling bond sites on the surface. The sticking cross section is then simply the ratio of the sticking cross section and the total area multiplied with the number of dangling bond sites.

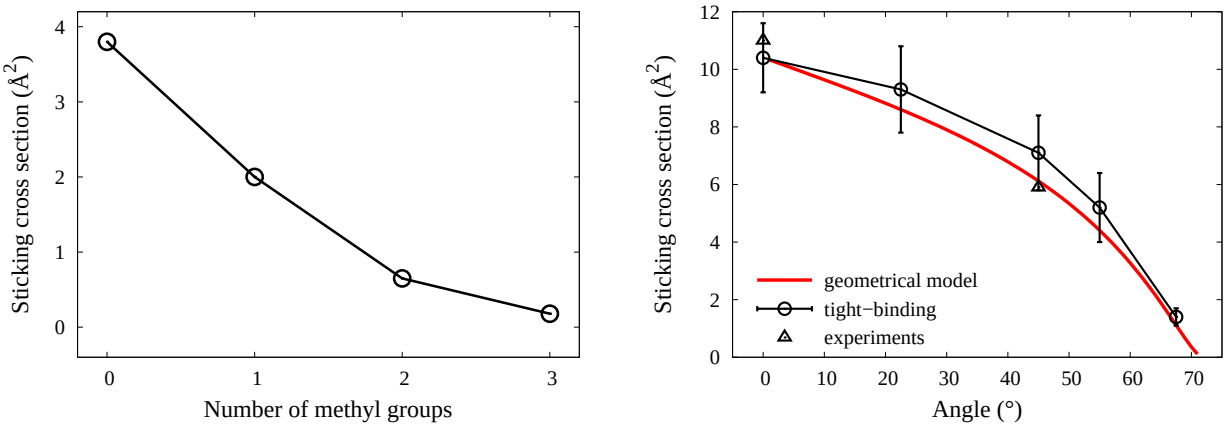

Figure 1: (a) Sticking cross sections obtained using the classical Brenner hydrocarbon potential and a surface with zero, one, two and three methyl groups next to the unsaturated carbon atom. (b) Sticking cross sections obtained when employing the tight-binding model in the simulations for the case with one dangling bond at the surface and different angles of incidence of the incoming methyl radical. The results are compared with sticking cross sections obtained with the simple geometrical model, and with experimental data [16; 17; 18]. The methyl gas temperature was 2100 K in all cases in our simulations.

5.1 Sensitivity to neighborhood

Several different surface configurations were created and used in our simulations in order to examine the effect of the local neighborhood of the dangling bond on the sticking cross section. The cross section is observed to decrease with increasing number of methyl groups surrounding the dangling bond. In Fig. 1a the sticking cross section dependence of the local neighborhood is depicted.

Depending on the surface configuration, the sticking cross sections are observed to vary by two orders of magnitude. Although the configuration of three methyl radicals surrounding an unsaturated carbon site is quite improbable, this study illustrates the importance of the hydrogen flux on the growth of the C:H network. Without the removal of the hydrogen atoms bound in the methyl groups, the probability of CH_3 adsorption remains low.

5.2 Angular dependence

Depending on the angle of incidence, the sticking cross-section was observed to decrease from (10.4±1.2) to (1.4±0.3) Å^2 (see Fig. 1a), when the angle of incidence increased from 0° to 67.5° in our simulations. In publication **II**, a simple radially symmetric model was developed in order to explain this angular dependence. In this model, the surface region around an unsaturated carbon site

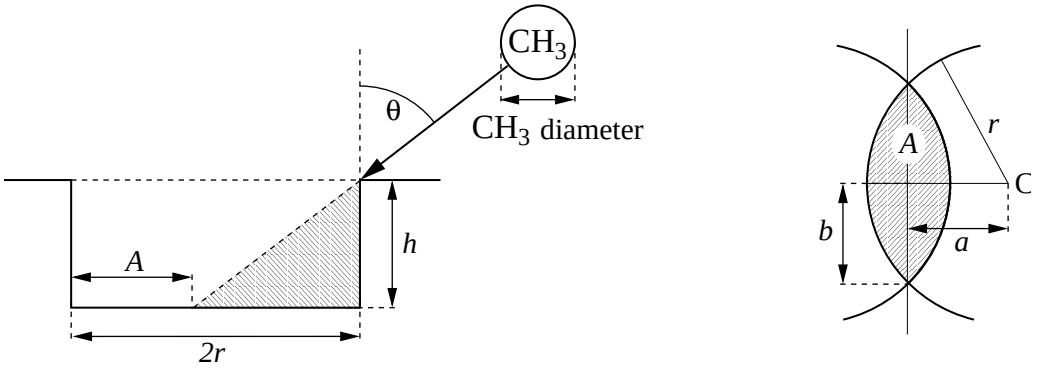

(a) side view (b) top view

Figure 2: (a) Simple geometrical model for the sticking cross section at a certain angle θ of incidence of the CH_3 radical. The cross section is calculated as the total area A at the bottom of the cylinder, where the incoming radical is able to chemisorb onto the dangling bond. (b) Calculation of the total area A (shaded) at the bottom of the dangling bond cylinder, in which radicals are able to chemisorb onto the unsaturated carbon atom. This area consists of two segments of two circles. a is defined as the distance from the center of the cylinder, C, to the point of intersection in the middle of the two circle segments. b is defined as the distance from this intersection to the point of intersection between the two circles.

is approximated by a cylinder with the surrounding hydrogen atoms forming its edges. We assume that the incoming radical is moving along a straight path, and that it can only change its direction via scattering from the surface. Radicals which reach the bottom of the cylinder are assumed to stick always. The area of the bottom of this cylinder, on which the incoming radical is able to chemisorb onto the dangling bond, thereby decreases with increasing angle of incidence.

The sticking cross-section $\sigma(\theta)$ is thus the total area not shadowed at the bottom of the dangling bond cylinder, A (see Fig. 2). Using geometry, this area is obtained as

$$A(r,h,\theta) = 2\tan^{-1}\left(\frac{\sqrt{r^2-a^2}}{a}\right) r^2 - 2a\sqrt{r^2-a^2}, \tag{1}$$

where

$$a = \frac{1}{2} h \tan(90-\theta). \tag{2}$$

An effective radius is first obtained for the CH_3 radical by calculating the total volume of one carbon and three hydrogen atoms from their covalent radii (0.77 Å for C and 0.35 Å for H), and then computing the radius of a sphere with this volume. The parameter h is then chosen as the sum of the effective

radius of the CH_3 radical (≈ 0.85 Å) and the covalent radius of a hydrogen atom (0.35 Å). This choice has the following physical motivation: if the carbon atom in the methyl radical gets down to the same level as the hydrogen atoms surrounding the unsaturated carbon site, there is nothing which prevents it from sticking. Otherwise it is assumed to be reflected. The parameter d, defined as $d = 2r$, is simply a fit to the sticking value for $\theta = 0$. This gives $r = 1.82$ Å and $h = 1.20$ Å. Note that the d parameter is the only fitted parameter in the model.

The geometrical model yields excellent agreement with the sticking coefficients observed in our TB MD simulations, see Fig. 1b. In particular, it gives a natural explanation why the sticking coefficient drops to almost exactly zero at 90° angle of incidence.

The simple geometrical model does not account for at least three processes related to sticking. First, the angle of rotation of the radical with respect to the surface has an effect on the sticking probability. A radical rotated such that its hydrogen atoms face the surface will react more easily with the surface as observed in our simulations. In the opposite case the methyl radical will more likely stick to the dangling bond. Second, some of the radicals that in the simple geometrical model would react with the dangling bond, can for example, also react with a surface hydrogen, resulting in the formation of a CH_4 molecule. Third, radicals have also been observed to chemisorb onto the unsaturated carbon atom when impinging at a rather large distance from the dangling bond. This is due to a steering effect, and leads to a larger sticking cross section. However, the fact that our radially symmetric model fits the angular dependence very well, indicates that all these complications can be averaged out as a first approximation.

5.3 Reaction processes

According to our simulations the following reaction mechanisms can occur. The most common reaction processes for the incoming CH_3 radical are (1) to chemisorb onto the dangling bond, or (2) to form a CH_4 molecule. In the latter case, the incoming CH_3 radical captures a hydrogen on the surface, and drifts away as a CH_4 molecule. Another reaction mechanism, is (3) the formation of a CH_2 molecule. In this case, one of the hydrogens in the CH_3 molecule chemisorbs onto the dangling bond, and the rest of the molecule drifts away as a CH_2 molecule. The formation of CH_2 molecules was observed to increase when the angle of incidence of the incoming CH_3 radical increases.

In addition, some unusual bonding configurations were also observed at the surface with seven dangling bonds. In some cases the CH_3 group fragmented as one or two of its hydrogen atoms chemisorbed to unsaturated carbon sites at the surface. The remaining CH_x group chemisorbed onto the surface, either onto another dangling bond site or by sticking to the surface between two dangling

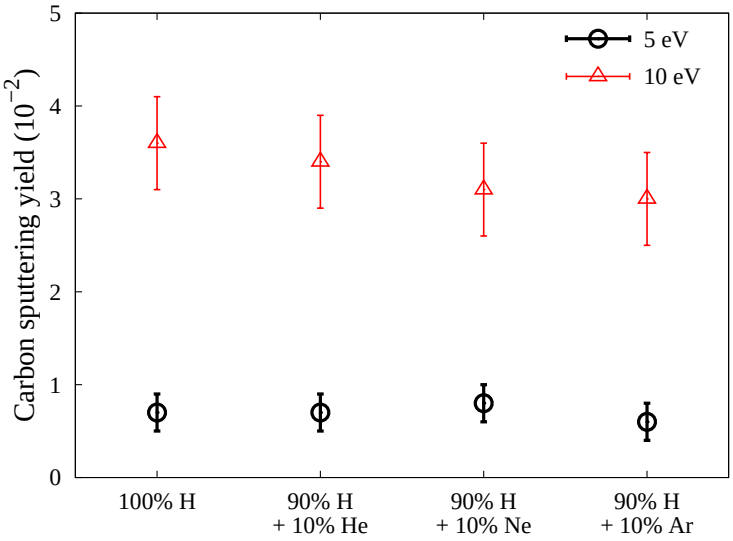

Figure 3: Carbon sputtering yields obtained from cumulative bombardment simulations of ions impinging at the following rates: 100% H, 90% H + 10% He, 90% H + 10% Ne, and 90% H + 10% Ar. Energies of the incident particles were 5 and 10 eV.

bond sites. These bonding configurations were probably intermediate and metastable, but the time scale of the simulations did not allow us to determine the lifetime of these states.

The above mentioned reaction mechanisms were only observed in the tight binding simulations. In the classical simulations only sticking of the CH_3 radical onto a dangling bond, or reflection of the same radical from the surface occurred.

6 EROSION

6.1 Noble gas effects

During device operation of a fusion reactor with carbon as the first wall material, these surfaces are eroded due to bombardment by not only low energy hydrogen ions, but also impurities. The most important of these impurities are noble gases, such as He, Ne, and Ar ions. Detailed knowledge about the evolution and hence the lifetime of the PFCs can be achieved by investigating the co-bombardment of amorphous hydrocarbon surfaces with hydrogen and noble gas ions. After performing cumulative bombardment simulations at a noble gas/hydrogen ratio of 1/10, and at energies of 5 and 10 eV, the erosion yields were calculated and compared for different noble gases. As shown in Fig. 3, at a ratio of 1/10 the sputtering yields obtained from simulations with different noble gas ions do not display any significant differences.

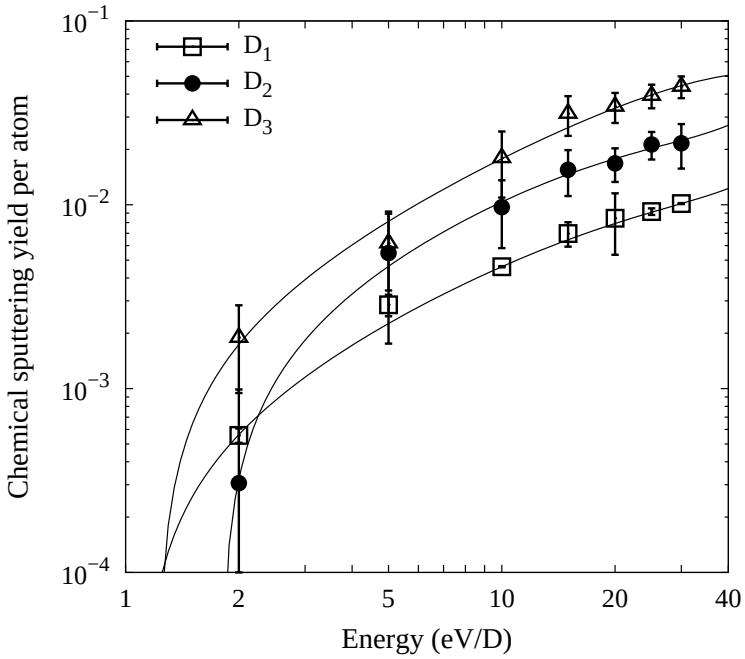

Figure 4: Simulation results for the chemical sputtering yields per atom of graphite (a-C:D) by incident D^+, D_2^+, D_3^+ projectiles. The data are averages over six different surfaces. The uncertainty is the standard error of the mean of the results obtained for the different surfaces. The solid lines have been drawn to guide the eye.

A marked difference in the morphology was, however, observed between results from the 5 and the 10 eV runs. This is also expressed in a large difference in the carbon sputtering yield. This indicates that the chemical erosion of carbon in fusion reactors may be more sensitive to the edge plasma temperature than previously assumed.

The analysis of the sputtered species during ion bombardment showed that sputtering of C_2H_x species dominates. This applies for both the 5 and the 10 eV case, although the erosion yield in the 5 eV case is much lower. During the first 500 cumulative simulation runs there occurred no erosion of larger (C_xH_y, where x > 4) carbon species. After this, that is after a saturated surface was obtained, we observed sputtering of considerably more high-molecular weight carbon C_xH_y species.

6.2 $\mathbf{D^+}$ *vs.* $\mathbf{D_2^+}$ *vs.* $\mathbf{D_3^+}$

The results from our simulations of 2 – 30 eV D^+ vs. D_2^+ vs. D_3^+ bombardment onto amorphous hydrocarbon surfaces are shown in Fig. 4. The experimental methane production yields overlap within experimental error for all three incident projectiles at 60 eV/D, and differ by less than a factor of two at the lowest measured energy of 10 eV/D. For the MD simulations, the total yield increases with the molecular weight.

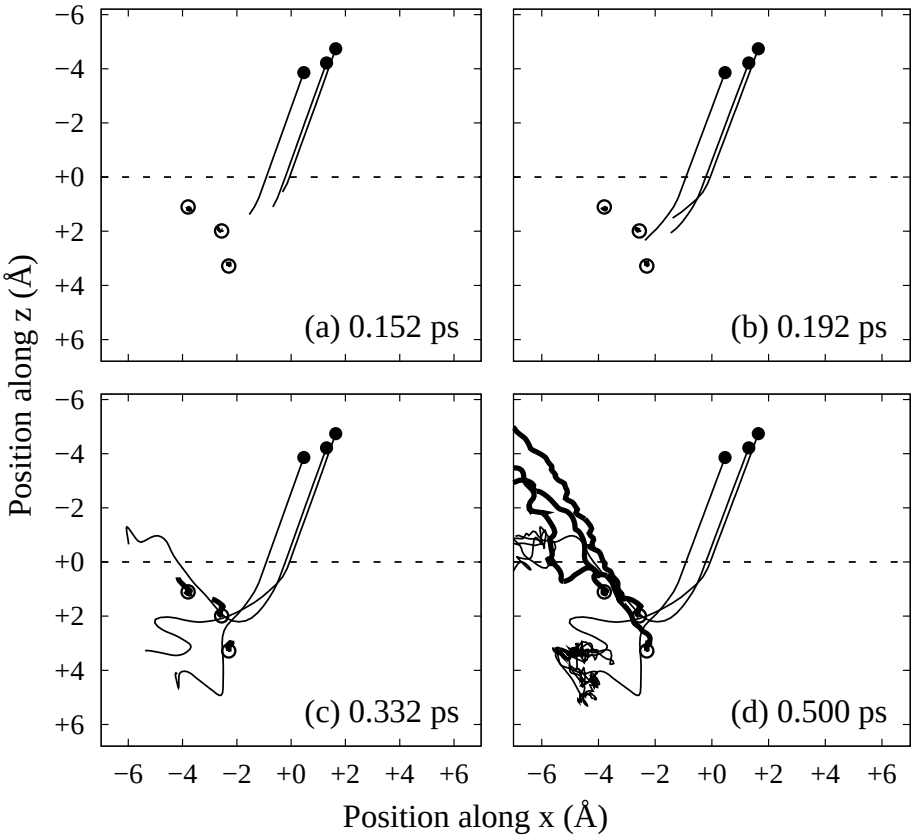

Figure 5: Trajectories of atoms in a 20 eV D_3 impact event leading to sputtering. For clarity, only the three incoming D atoms of the incident D_3^+ projectile and the three sputtered C atoms are shown. The initial positions of the three D atoms and the C atoms are shown with solid and open circles, respectively. The D and C trajectories are shown with thin and thick lines, respectively. Each frame shows the trajectories up to the time indicated in the lower right corner.

An extended study of the time evolution of trajectories of both D atoms of an incoming D_3 projectile and sputtered C atoms in individual MD simulations showed that in a significant fraction of the events, which lead to sputtering, the D atoms remain bound or close to each other (see Fig. 5). These results strongly suggest that a major part of the differences in the yields for the different beams (D^+, D_2^+, and D_3^+) can be explained by classical energy-transfer processes, which contribute to the kinetic desorption of the erosion precursors.

This effect may, at last in part, explain the differences in isotope effects observed by Mech *et al.* and Roth and co-workers. Using H_3^+ and D_2^+ beams (Mech *et al.*), the increase in maximum energy transfer is only about 2.4%, while in the case of H_3^+ and D_3^+ (Roth *et al.*) the maximum energy transfer increase is more than an order of magnitude larger (33.5 %). The possibility of intact molecular projectiles enhancing kinetically assisted desorption of erosion products from graphite surface can, therefore, interfere with the isolation and quantitative assessment of other projectile-mass-related

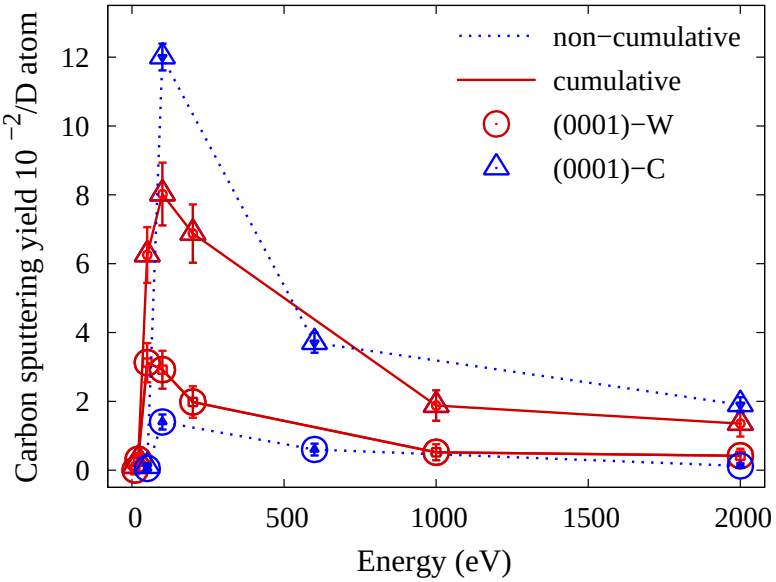

Figure 6: Carbon sputtering yields calculated obtained from cumulative and non-cumulative bombardment simulations of deuterium impinging onto crystalline sample cells of tungsten carbide. The sputtering of tungsten is practically negligible.

effects such as the H/D/T isotope effect. For unambiguous identification and quantification of the latter effect, the use of atomic projectiles is thus highly recommended.

6.3 Tungsten-carbide

The carbon sputtering yields obtained from the cumulative simulations of (0001)-W and (0001)-C surfaces are shown in Fig. 6. Both surfaces display the same trend: The yield rises from close to zero at low bombardment energies, peaks for 100 eV, and thereafter decreases with increasing ion energy. For all energies the erosion of tungsten is practically negligible which is equivalent to a preferential sputtering of carbon and in agreement with experiment (see below). The difference between the simulations of the (0001)-W and (0001)-C surfaces is small. The yields are slightly larger in the (0001)-C case, since carbon atoms in the first surface layer react more easily with the incoming deuterium ions.

It is noteworthy that some erosion occurs for all energies, even at an energy of only 10 eV. The maximum possible energy transfer from a 10 eV D to C is only 4.9 eV. This is much less than the cohesive energy of C in bulk WC, which implies that ordinary physical sputtering of carbon cannot account for the observed erosion. Visual inspection of the evolution of the simulation cells during bombardment provides an explanation for this observation. Erosion of carbon and carbon containing molecules is more significant for the carbon terminated surface because of swift chemical sputtering

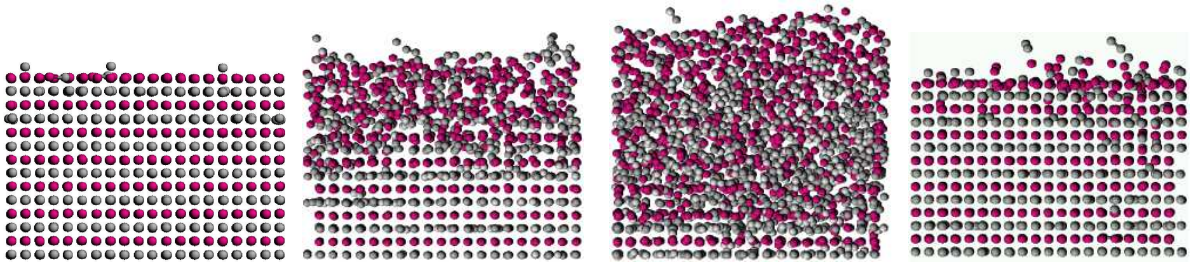

(a) 10 eV (b) 50 eV (c) 100 eV (d) 1 keV

Figure 7: Snapshots of the the last frames of the WC lattice after cumulative deuterium bombardment with 2000 ions at (a) 10 eV, (b) 50 eV, (c) 100 eV, and (d) 1 keV. The lighter spheres represent C atoms and the darker ones W atoms.

[45; 46; 47], which is known to govern erosion at energies below the threshold for physical sputtering. Note that on the C-terminated WC surface, the C atoms have only 3 bonds to the underlying W layer (the C atoms are too far from each other to have covalent bonds with each other). These three bonds can be broken by swift chemical sputtering. Our present results show that the threshold for carbon erosion from tungsten carbide due to deuterium by this mechanism is less than 10 eV.

Snapshots of the cells at the end of the cumulative simulations reveal that the surfaces are amorphized at energies between about 50 eV and 200 eV. The amorphization is the most pronounced at an energy of 100 eV corresponding to the maximum in the yield (see Fig. 7). During the course of the simulation, carbon molecules formed due to amorphization of the surface are subject to erosion by swift chemical sputtering [45; 46]. For energies below about 50 eV and above 200 eV the crystalline structure remains largely intact. Energies below 50 eV are obviously too small to cause non-recoverable damage. On the other hand, for energies above about 200 eV the maximum of the depth distributions of the energy and the deposited ions exceed the height of the simulation cells used in the current simulations.

In both cumulative as well as non-cumulative simulations, the W sputtering yield is very low ($\ll$ 0.01). This implies that C is sputtered preferentially. The preferential sputtering of C naturally leads to W enrichment at the surface. The calculated W surface concentration as a function of ion fluency shows excellent agreement with the W surface concentration during 300 eV D bombardment, using Auger electron spectroscopy, as measured by Plank and Eckstein [19].

Our observation of large C sputtering yields from WC during D bombardment conform with the swift chemical sputtering mechanism. This mechanism is important in a relatively narrow energy window [47]. On the other hand, the W yields remain low since W is a metal which prefers high coordination numbers and hence does not easily sputter by the swift chemical sputtering mechanism. The physical sputtering yields for W by D are experimentally known to be very low ($\ll$ 0.01) in pure tungsten [48].

Since W and WC have comparable cohesive energies, the physical sputtering yield of W from WC can be expected to be comparably small, which is consistent with our simulation results.

7 SUMMARY

Carbon, carbon based materials, tungsten, and beryllium are presently considered as potential materials for plasma facing components in fusion reactors. In devices with carbon based first walls, hydrocarbon molecules are sputtered due to intense bombardment of hydrogenic particles, and layers with redeposited hydrocarbons are observed to form, not only on the divertor plates, but also in remote regions of the vacuum chamber. In order to obtain control over the tritium inventory bound in the deposited hydrocarbon films, detailed knowledge about the properties and the growth of hydrocarbon films is required. In this thesis, molecular dynamics simulations based both on a semi-empirical tight-binding method and empirical force models have been employed to gain detailed information about the sticking and erosion of ions and molecules at these surfaces.

The investigations on sticking of methyl radicals onto unsaturated carbon sites on diamond (111) surfaces revealed that the local neighborhood of a dangling bond can lead to a variation of the sticking cross section over two orders of magnitude. The sticking cross section of methyl radicals was also observed to depend on the angle of incidence. This dependence can be described by a simple geometrical model.

The behavior of amorphous hydrogenated carbon surfaces under co-bombardment with hydrogen and noble gas atoms was studied for energies of 5 and 10 eV. Within statistical uncertainty, the erosion yields were the same for different noble gas ions. A marked difference in the surface morphology, however, was observed for different ion energies. This indicates that the chemical erosion of carbon in fusion reactors is probably more sensitive to the edge plasma temperature than previously assumed.

The sputtering yields obtained from simulations of D^+, D_2^+, and D_3^+ ions impinging onto hydrocarbon surfaces at energies between 2 and 30 eV, showed that molecular projectiles can lead to larger yields per atom than atomic projectiles. This indicates that the simple scaling approximation which has been used to deduce data for atomic projectiles from experiments using molecular projectiles is not sufficient and additional corrections need to be taken into account.

Prolonged bombardment of tungsten carbide surfaces by deuterium ions was shown to lead to the formation of an amorphous WC surface layer, regardless of the initial structure of the simulation cell. Erosion of carbon is dominant for both carbon and tungsten terminated surfaces. Just like carbon-based materials, WC-like materials can, hence, be expected to be subject to chemical erosion down

to very low energies of impinging deuterium or tritium particles. This is in contrast to pure tungsten, which does not erode due to chemical sputtering.

In agreement with experiment, preferential sputtering of carbon was observed in the simulations. This suggests that WC layers formed by carbon redeposition will be reduced in carbon content if they are subjected to continued hydrogen/deuterium bombardment. Hence, if a section of the reactor first wall is subject to both redeposition of hydrocarbons and hydrogen bombardment, a dynamic balance in the carbon content will be reached under prolonged operation.

ACKNOWLEDGMENTS

I wish to thank the current and former heads of the laboratory, Prof. Jyrki Räisänen and Doc. Eero Rauhala, for providing the facilities of the laboratory to my disposal. I also thank Prof. Juhani Keinonen, the head of the Department of Physical Sciences, for the opportunity to conduct research at the department, and for his advice and help during this work.

Special thanks are due to my supervisor Prof. Kai Nordlund for inspiration, many valuable discussions and his expert guidance to the world of computational and materials physics. I am indebted to Dr. Emppu Salonen who helped me to take the first steps in the area of atomistic simulations and fusion related research. Warm thanks are due to Prof. Chung Wu and Dr. Arkady Krasheninnikov for fruitful discussions and collaboration in our studies.

Thanks are due to co-workers and colleagues at the laboratory and the department.

Warm thanks to my family and friends and especially to Paul for constant support and encouragement through the years.

Financial support from the Academy of Finland and Magnus Ehrnrooth's Foundation is gratefully acknowledged.

Helsinki, July 24, 2006
Petra Träskelin

References

1. More information on the fusion technology research and development can be found at the ITER web page, http://www.iter.org.

2. C. H. Wu, C. Alessandrini, R. Moormann, M. Rubel, and B. M. U. Scherzer, *Evaluation of silicon doped CFCs for plasma facing material*, J. Nucl. Mater. **220-222**, 860 (1995).

3. V. Barabash, G. Federici, R. Matera, A. R. Raffray, and ITER Home Teams, *Armour materials for the ITER plasma facing components*, Physica Scripta **T81**, 74 (1999).

4. G. Federici, R. A. Anderl, P. Andrew, J. N. Brooks, R. A. Causey, J. P. Coad, D. Cowgill, R. P. Doerner, A. A. Haasz, G. Janeschitz, W. Jacob, G. R. Longhurst, R. Nygren, A. Peacock, M. A. Pick, V. Philipps, J. Roth, C. H. Skinner, and W. R. Wampler, *In-vessel tritium retention and removal in ITER*, J. Nucl. Mater. **266-269**, 14 (1999).

5. J. Roth, *Chemical erosion of carbon based materials in fusion devices*, J. Nucl. Mater. **266-269**, 51 (1999).

6. R. Parker, G. Janeschitz, H. D. Pacher, D. Post, S. Chiocchio, G. Federici, P. Ladd, ITER Joint Team, and Home Teams, *Plasma-wall interactions in ITER*, J. Nucl. Mater. **241-243**, 1 (1997).

7. in *CRC Handbook of Chemistry and Physics, 76th ed.*, edited by D. R. Lide (CRC Press, Boca Raton, FL, USA, 1995).

8. G. Janeschitz and ITER JCT and HTs, *Plasma-wall interaction issues in ITER*, J. Nucl. Mater. **290-293**, 1 (2001).

9. W. Wang, J. Roth, S. Lindig, and C. H. Wu, *Blister formation of tugsten due to ion bombardment*, J. Nucl. Mater. **299**, 124 (2001).

10. E. Hechtl, H. R. Yang, C. H. Wu, and W. Eckstein, *An experimental study of tungsten self sputtering*, J. Nucl. Mater. **176 & 177**, 874 (1990).

11. W. Eckstein and J. László, *Sputtering of tungsten and molybdenum*, J. Nucl. Mater. **183**, 19 (1991).

12. Y. Hirooka, *Review of beryllium and tungsten erosion and universal modeling of plasma impurity effects observed in recent PISCES experiments*, Physica Scripta **T64**, 84 (1996).

13. C. H. Wu and U. Mszanowski, *A comparison of lifetimes of beryllium, carbon, molybden and tungsten as divertor armour materials*, J. Nucl. Mater. **218**, 293 (1995).

14. J. Küppers, *The hydrogen surface chemistry of carbon as a plasma facing material*, Surf. Sci. Rep. **22**, 249 (1995).

15. P. Andrew *et al.*, *Tritium recycling and retention in JET*, J. Nucl. Mater. **266-269**, 153 (1999).

16. A. von Keudell, *Formation of polymer-like hydrocarbon films from radical beams of methyl and atomic hydrogen*, Thin Solid Films **402**, 1 (2002).

17. M. Meier and A. von Keudell, *Hydrogen elimination as a key step for the formation of polymerlike hydrocarbon films*, J. Appl. Phys. **90**, 3585 (2001).

18. M. Meier, R. Preuss, and V. Dose, *Interaction of CH_3 and H with amorphous hydrocarbon surfaces: estimation of reaction cross sections using Bayesian probability theory*, New J. of Phys. **133**, 1 (2003).

19. H. Plank and W. Eckstein, *Preferential sputtering of carbides under deuterium irradiation - a comparison between experiment and computer simulation*, Nucl. Instr. Meth. Phys. Res. B **124**, 23 (1997).

20. W. Wang, V. K. Alimov, B. M. U. Scherzer, and J. Roth, *Deuterium trapping in and release from tungsten carbide*, J. Nucl. Mater. **241-243**, 1087 (1997).

21. M. I. Guseva, A. L. Suvorov, S. N. Korshunov, and N. E. Lazarev, *Sputtering of beryllium, tungsten, tungsten oxide and mixed W-C layers by deuterium ions in the near-threshold energy range*, J. Nucl. Mater. **266-269**, 222 (1999).

22. M. I. Guseva, S. N. Korshunov, A. L. Suvorov, and N. E. Lazarev, *Sputtering of tungsten, tungsten oxide, and tungsten-carbon mixed layers by deuterium in the threshold energy region*, Tech. Phys. **44**, 1123 (1999).

23. M. Tanihuchi, K. Sato, K. Ezato, K. Yokoyama, M. Dairaku, and M. Akiba, *Sputtering of carbon-tungsten mixed materials by low energy deuterium*, J. Nucl. Mater. **313-316**, 360 (2003).

24. W. Eckstein, *Computer simulations of ion solid interactions* (Springer, Berlin/Heidelberg, Germany, 1992), vol. 10 of Springer Series in Materials Science.

25. D. W. Brenner, *Empirical potential for hydrocarbons for use in simulating the chemical vapor deposition of diamond films*, Phys. Rev. B **42**, 9458 (1990).

26. D. Porezag, T. Frauenheim, T. Kohler, G. Seifert, and R. Kaschner, *Construction of tight-binding-like potentials on the basis of density-functional theory: Application to carbon*, Phys. Rev. B **51**, 12947 (1995).

27. M. Elstner, D. Porezag, G. Jungnickel, J. Elsner, M. Haugk, T. Frauenheim, H. Suhai, and G. Seifert, *Self-consistent-charge density-functional tight-binding method for simulations of complex materials properties*, Phys. Rev. B **58**, 7260 (1998).

28. B. J. Alder and T. E. Wainwright, *Phase transition for a Hard Sphere-System*, J. Chem. Phys. **27**, 1208 (1957).

29. K. Nordlund, *Molecular dynamics simulation of ion ranges in the 1 - 100 keV energy range*, Comput. Mater. Sci. **3**, 448 (1995).

30. J. Tersoff, *New empirical approach for the structure and energy of covalent systems*, Phys. Rev. B **37**, 6991 (1988).

31. J. Tersoff, *Empiric interatomic potential for carbon, with applications to amorphous carbon*, Phys. Rev. Lett. **61**, 2879 (1988).

32. H. U. Jäger and M. Weiler, *Molecular dynamics studies of a-C:H film growth by energetic hydrocarbon molecule impact*, Diamond Rel. Mater. **7**, 858 (1998).

33. W. Zhu, Z. Pan, Y. Ho, and Z. Man, *Impact-induced chemisorption of C_2H_2 on diamond(001) surfaces: a molecular dynamics simulation*, Nucl. Instr. Meth. Phys. Res. B **153**, 213 (1999).

34. R. Smith and K. Beardmore, *Molecular dynamics studies of particle impacts with carbon-based materials*, Thin Solid Films **272**, 255 (1996).

35. A. Krasheninnikov, K. Nordlund, M. Sirviö, E. Salonen, and J. Keinonen, *Formation of ion irradiation-induced atomic-scale defects on walls of carbon nanotubes*, Phys. Rev. B **63**, 245405 (2001).

36. H. U. Jäger and K. Albe, *Molecular-dynamics simulations of steady-state growth of iondeposited tetrahedral amorphous carbon films*, J. Appl. Phys. **88**, 1129 (2000).

37. A. Krasheninnikov, K. Nordlund, E. Salonen, and J. Keinonen, *Sputtering of amorphous hydrogenated carbon by hyperthermal ions as studied by tight-binding molecular dynamics*, Comput. Mater. Sci. **25**, 427 (2002).

38. J. F. Ziegler, J. P. Biersack, and U. Littmark, *The stopping and range of ions in matter* (Pergamon, New York, U.S.A., 1985).

39. N. Juslin, P. Erhart, P. Träskelin, J. Nord, K. Henriksson, E. Salonen, K. Nordlund, and K. Albe, *Analytical interatomic potential for modeling non-equilibrium processes in the W-C-H system*, J. Appl. Phys. **98**, 123520 (2005).

40. C. M. Goringer, D. R. Bowler, and E. Hernandez, *Tight-binding modelling of materials*, Rep. Prog. Phys. **60**, 1447 (1997).

41. T. Frauenheim, P. Blaudeck, U. Stephan, and G. Jungnickel, *Atomic structure and physical properties of amorphous carbon and its hydrogenated analogs*, Phys. Rev. B **48**, 4823 (1993).

42. U. Stephan, T. Frauenheim, P. Blaudeck, and G. Jungnickel, π - *bonding versus electronic defect generation: an examination of band gap properties in amorphous carbon*, Phys. Rev. B **50**, 1489 (1994).

43. H. J. C. Berendsen, J. P. M. Postma, W. F. van Gunsteren, A. DiNola, and J. R. Haak, *Molecular dynamics with coupling to external bath*, J. Chem. Phys. **81**, 3684 (1984).

44. V. Philipps, E. Vietzke, and K. Flaskamp, *Sticking probabilities of evaporated C_1, C_2, C_3 on pyrolytic graphite*, Surf. Sci. **178**, 806 (1996).

45. E. Salonen, K. Nordlund, J. Keinonen, and C. H. Wu, *Bond-breaking mechanism of sputtering*, Europhysics Letters **52**, 504 (2000).

46. E. Salonen, K. Nordlund, J. Keinonen, and C. H. Wu, *Swift chemical sputtering of amorphous hydrogenated carbon*, Phys. Rev. B **63**, 195415 (2001).

47. A. V. Krasheninnikov, E. Salonen, K. Nordlund, J. Keinonen, and C. H. Wu, *Tight-binding atomistic simulations of carbon sputtering by hyperthermal ions in tokamak divertors*, Contrib. Plasma Phys. **42**, 451 (2002).

48. R. Behrisch (ed.), *Sputtering by Particle bombardment I* (Springer, Berlin, 1981).